International Journal of Biological Macromolecules 240 (2023) 124459

Contents lists available at ScienceDirect

International Journal of Biological Macromolecules

journal homepage: www.elsevier.com/locate/ijbiomac

Modification of hyaluronic acid to enable click chemistry photo-crosslinking of hydrogels with tailorable degradation profiles

Ciara Buckley [a], Therese R. Montgomery [b], Tomasz Szank [c], Brian A. Murray [d], Cormac Quigley [b], Ian Major [a,*]

[a] PRISM Research Institute, Technological University of the Shannon, Athlone N37 HD68, Ireland
[b] School of Science and Computing, Atlantic Technological University, Galway H91 T8NW, Ireland
[c] Biosciences Research Institute, Technological University of the Shannon, Athlone N37 HD68, Ireland
[d] Department of Science, Technological University Dublin- Tallaght Campus, Dublin D24 FKT9, Ireland

ARTICLE INFO

Keywords:
Hyaluronic acid
Photopolymerisation
Click-chemistry

ABSTRACT

Hyaluronic acid (HA) is a naturally occurring mucopolysaccharide that, due to its inherent bioactivity and extracellular matrix-like structure, has the potential to be utilised extensively in tissue engineering. However, this glycosaminoglycan lacks the properties required for cellular adhesion and photo-crosslinking by UV light, which significantly hinders this polymers applicability. This research presents a method for modifying hyaluronic acid via thiolation and methacrylation to generate a novel photo-crosslinkable polymer with improved physicochemical properties, biocompatibility and the potential to customize biodegradability according to the ratio of monomers used. A decrease in stiffness proportional to increasing thiol concentration was observed when testing the compressive strength of hydrogels. Conversely, it was noted that the storage moduli of hydrogels increased proportionally to thiol concentration indicating a greater degree of cross-linking with the addition of thiol. The addition of thiol to HA increased the biocompatibility of the material in both neuronal and glial cell lines and improved the degradability of methacrylated HA. Due to the enhanced physicochemical properties and biocompatibility imparted by the introduction of thiolated HA, this novel hydrogel system could have numerous bioengineering applications.

1. Introduction

Hyaluronic acid (HA) is a naturally occurring mucopolysaccharide that belongs to the glycosaminoglycans (GAGs) family of heteropolysaccharides. GAGs have multiple functions in the human body, including roles in cell development and proliferation [1] and wound healing [2]. Due to their essential roles in the extracellular matrix, many GAGs, such as heparin sulfate and HA, are of great interest as biomaterials. Interestingly, HA is the only GAG that lacks sulfation and, as a result, cannot bind to a core protein to create a proteoglycan [3]. HA is created endogenously in the human body and is present in all bodily fluids, from synovial fluid to urine [4]. It is this endogenous character that makes it of particular interest over polymers with similar properties such as chitosan or pectin. Certain bacterial species, such as Streptococcus, have evolved the ability to synthesize HA; nevertheless, the presence of endotoxins renders them an undesirable and laborious source of HA for industrial purposes. Biotechnological production of HA primarily utilizes genetically modified strains of Lactobacillus, which, unlike Streptococcus, do not create endotoxins and are generally regarded as safe (GRAS) [5].

Due to its unique viscoelastic properties, HA has been at the forefront of biomaterials for many years [6]. These properties enable the use of HA in a variety of forms, from microgels [7], nanogels [8], and cryogels [9] to nanoparticle conjugates [10]. In addition, HA has an exceptional ability to bind water, which permits a variety of applications ranging from topical to injectable hydrogels [11]. Native HA is easily degraded by endogenous enzymes known as hyaluronidases, which is a significant limitation [12]. These enzymes cleave the glycosidic bond, degrading the HA polysaccharide from a high-molecular-weight (HMW) chain to low-molecular-weight (LMW) oligos (10 kilodaltons (kDa)) that have very different effects on the body. Numerous investigations have demonstrated that HMW HA (>1000 kDa) has anti-immunogenic and anti-angiogenic effects, whereas LMW HA is immune-stimulatory and pro-angiogenic [13,14]. Due to the viscosity exhibited even at low concentrations, HMW HA can be difficult to work with depending on the

* Corresponding author.
E-mail address: ian.major@tus.ie (I. Major).

https://doi.org/10.1016/j.ijbiomac.2023.124459
Received 22 December 2022; Received in revised form 16 March 2023; Accepted 11 April 2023
Available online 16 April 2023

Abbreviations

HA	Hyaluronic acid
GAG	Glycosaminoglycan
kDa	Kilodalton
HMW	High molecular weight
LMW	Low molecular weight
FBS	Foetal Bovine Serum
PBS	Phosphate Buffered Saline
NEAAs	Non-essential Amino Acids
Pen-Strep	Penicillin-Streptomycin
MWCO	Molecular weight cut off
MoD	Degree of modification
PDL	Poly-D-Lysine
UV	Ultraviolet
wv	Weight per volume
IR	Infrared
RP-HPLC	Reversed phase High Performance Liquid Chromatography
DNTB	5,5′-dithio-bis(2-nitrobenzoic acid)

application. For this reason, there has been a great deal of interest in using moderate molecular weight HA (50–500 kDa), which has the advantages of low molecular weight HA, such as penetration through skin, proliferation and migration of vascular endothelial cells, and wound healing abilities [4,15,16], whilst simultaneously proving more amenable to engineer. In this study, the molecular weight of HA chosen was 30–50 kDa to enable ease of modification, retain printability and the ability to pipette the polymer when in solution. This biopolymer can be modified in a variety of ways, as discussed in detail by Buckley et al. [4], Schanté et al. [17], and Huang and Chen [18], in order to extend or alter the residence time of HA in the body [19], and to add to the ever-expanding list of applications of HA [18].

Modification of the HA molecule can promote cross-linking and engineering of the molecule, modulation of enzymatic HA degradation, enhancement of cell adhesion [20,21]), and enable conjugation [22]. Native HA lacks the necessary adhesion sites for cell adhesion and therefore can display cytotoxic like effects when assayed which can hinder the preclinical testing stages of medical devices [23]. By modifying HA, this polymer can be engineered to be a cell supportive construct [24]. The relative simplicity of HAs structure facilitates the modification of any of its three major functional groups — hydroxyl, carboxyl, or acetyl. Once HA has been modified, it can be cross-linked to enable the building of structures suited for wound repair, nerve regeneration, or cell delivery [25]. A caveat to this, however, is that every change in structure will have an influence on biological functionality, whether through enzyme recognition or receptor recognition. The degree of modification specifically affects one of HA's key receptors, CD44. CD44 is thought to play a crucial role in pericellular matrix assembly and structure, and is necessary for cell attachment, proliferation, and wound repair [26]. To preserve CD44 functionality, it is recommended to limit the degree of alteration of the HA polymer to approximately 20 % [27]. Additionally, it should be noted that environmental factors will not only affect the degree of modification of the polymer but may also fragment the HA polysaccharide. Factors of importance include temperature, solvent and pH. For these reasons, all reactions were performed at ambient temperature, using water as a solvent and the pH was continuously monitored for both reactions.

HA can be modified via thiolation, which is accomplished via an amidation process. This reaction involves the activation of the carboxyl group of HA through carbodiimide. Other commonly used modification reactions for HA have been discussed in detail previously [4]. Adding a thiol group to a biopolymer such as HA enables crosslinking through click reactions. Click reactions are preferable to conventional free-radical photopolymerisation because they proceed under moderate conditions with greater efficiency, selectivity, faster kinetics, and insensitivity to oxygen and water [28]. These reactions occur in the presence of UV or visible light and minute amounts of photoinitiator, which is often a radical photoinitiator such as Irgacure 2959 due to its exceptional biocompatibility. However, native HA lacks the architecture necessary to facilitate click-chemistry reactions. For this reason, researchers have investigated numerous ways to introduce functional groups which can be manipulated in ways such as click chemistry reactions. In a study by Cadamuro et al. [29], HA was cross-linked with elastin by first functionalising both molecules with maleimide groups and then cross-linked with a dithiol PEG linker. The methodology used was very similar and for a similar end purpose, however, our study benefits from being self-contained in that no linker is required and the click chemistry reaction occurs between two functionalised HA molecules, resulting in a tunable HA hydrogel. In this study, click chemistry was used to cross-link thiolated HA (HA-SH) with methacrylated HA (HA-MA) to develop a hydrogel with superior physical and biological properties compared to methacrylated HA hydrogels alone. The structures of native HA, and the HA derivatives are illustrated in Fig. 1 below.

The primary hypothesis of the present investigation was that a UV photo-crosslinked hydrogel could be generated via thiolene chemistry by thiolating and methacrylating different batches of HA and mixing them in the presence of a photo-initiator and UV light. Due to the ratio of derivatives used, these click chemistry-produced hydrogels would have a customisable degradability profile and mechanical properties, and would consequently have several bioengineering uses.

2. Materials and methods

2.1. Materials

Hyaluronic acid (HA) (MW = 30–50 kDa), 4-Dimethylaminopyridine (DMAP), *N*-ethyl-*N*-(3-dimethylaminopropyl)carbodiimide hydrochloride (EDC HCl), cysteamine HCl and formamide were purchased from Glentham UK Ltd. DMEM (D5671) media, Poly-D-lysine (PDL), Foetal Bovine Serum (FBS), Penicillin-Streptomycin (Pen-Strep), L-glutamine, Trypsin, phosphate buffered saline (PBS), Neutral red, molecular grade ethanol, acetic acid, concentrated sulfuric acid, carbazole reagent, sodium tetraborate, methacrylic anhydride, sodium hydroxide pellets and resazaurin salt were purchased from Merck, Ireland. The UV curing system used was from Dr. Gröbel UV-Electronik GmbH, Ettlingen, Germany.

2.2. Preparation of HA derivatives

2.2.1. Cysteamine modified HA

Thiolated HA (HA-SH) was obtained by reacting a 2%wv solution of HA in deionised water with molar equivalents of EDC (0.77%wv) and DMAP (0.6089%wv) on ice to activate the carboxyl moiety. All molar equivalents were calculated on the basis of starting moles of HA used. After one hour, a 2-M equivalent of cysteamine HCl (1.1325%wv) in formamide was added dropwise under nitrogen gas and the reaction was allowed to proceed overnight, at pH 5, protected from light.

The resulting solution was dialysed (Molecular weight cut off (MWCO): 12–14 kDa) against 100 mM NaCl solution for 24 h with water changes every 4 h, followed by a further 24 h in acidified water with water changes every 4 h.

The dialysate was vacuum filtered before lyophilisation and storage at −20 °C until needed. Product yield was consistently 90 ± 5 %.

2.2.2. Methacrylate modified HA

Methacrylated HA (HA-MA) was initially prepared by reacting a 2% wv solution of HA in deionised water with molar equivalent (0.7684% wv), 10-fold (7.6838%wv) and 30-fold (23.0508%wv) molar excess of

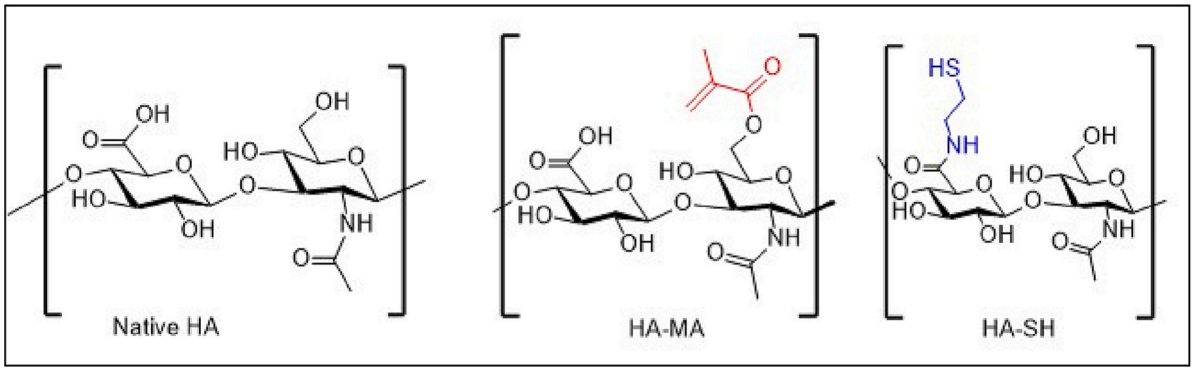

Fig. 1. Chemical structures of native HA, HA-MA and HA-SH.

methacrylic anhydride (MA). After calculating the degree of modification each molar ratio produced, subsequent reactions were performed using a 10-fold molar excess of MA. The reaction was adjusted to pH 8.5 with 5 M NaOH. Once the reaction had completed, the solution was dialysed (MWCO: 12–14 kDa) against basic water (pH 10) for 24 h with water changes every 4 h, followed by 24 h against deionised water with water changes every 4 h. The resulting dialysate was vacuum filtered before lyophilisation and storage at −20 °C until needed.

2.2.3. Cell lines

The cell lines utilised throughout this study were SH-SY5Y, a human neuroblastoma cell line, and RT4-D6P2T, a rat glial cell line. Frozen stocks were used to ensure a low passage number of both cell lines and the cells were stored at 37 degrees in a 95 % oxygen, 5 % CO_2 incubator. SH-SY5Y and RT4 D6P2T cells were maintained at a confluence of approximately 70 % for optimal performance. SH-SY5Y cells were passaged twice weekly using DMEM supplemented with 10 % FBS, 1 % L-glutamine, 1 % Pen-Strep and 1 % Non-essential amino acids (NEAAs). RT4 D6P2T cells were passaged twice weekly using DMEM supplemented with 10 % FBS, 1 % L-glutamine and 1 % Pen-Strep. SH-SY5Y is a catecholaminergic neuroblastoma cell line of human origin, it is because of this that SH-SY5Y is the most commonly used continuous cell line for Parkinson's research [30]. RT4 D6P2T is a rat schwannoma cell line and has been found to be the most similar in vitro model to myelinating Schwann cells [31]. For the purpose of this study, from here on SH-SY5Y will be referred to as the neuronal cell line and RT4 D6P2T will be referred to as the glial cell line.

2.2.4. Cytotoxicity of HA derivative blends

The cytotoxicity of HA and HA derivative blends was determined in SH-SY5Y and RT4 D6P2T cell lines. The cell viability (% of control, where control = cells with no treatment) was assessed using the resazaurin reduction assay as previously described [32] and the neutral red uptake assay as utilised by [33]. Both cell lines were propagated and maintained until reaching suitable confluence and passage number. 24 well tissue culture plates were coated in the HA derivative concentrations (0, 0.001, 0.01, 0.1, 0.5, 1%wv) dissolved in 0.1 mg/ml poly-D-lysine (PDL) before seeding SH-SY5Y (0.5×10^6 cells/ml) and RT4 D6P2T (0.25×10^6 cells/ml) cells and incubating for 20 h. After incubation, resazaurin (0.05%wv) or neutral red (0.004%wv) was added to the treated cells and incubation continued for a further 4/ 3 h respectively. After incubation, the resazaurin reduction assay plate was analysed using fluorescent spectrometry at an excitation/ emission (ex/em) of 530/ 590. The neutral red uptake absorbance was read at 540 nm after destaining with a 1%wv acetic acid in 50%*v*/v ethanol solution using a microplate reader (Bruker). Cell viability was determined as the relative percentage of treated cells to the untreated (control) cells.

2.3. UV cross-linking of HA derivative blends

HA hydrogels of varying composition were created as outlined in Table 1 below. A 5%wv solution was prepared of both HA-SH and HA-MA before composing the various blends. Irgacure 2959 was prepared as a methanolic stock with a final concentration in each hydrogel of 0.1%wv. The solution was placed in a silicone mould and photopolymerisation was performed using a UV curing system with a controlled radiation source consisting of 20 UV-tubes in the spectral range of 315–400 nm at an average intensity of 10–13.5 mW/cm^2. A period of 10 min was found to be optimal for polymerisation through a series of preliminary studies not reported here, after which time it was determined whether polymerisation was successful or not.

2.4. Attenuated total reflectance-Fourier transform infrared (ATR-FTIR) spectroscopy

ATR-FTIR was performed to analyse the chemical changes in cross-linked samples after photopolymerisation. IR spectra were recorded in transmittance mode with an FT-IR spectrometer (Perkin Elmer, Waltham, MA, USA) at 21 °C in the spectral range 4000–650 cm^{-1}, utilising a compression force of 80 N on all samples. Samples were tested in quintuplicate ($N = 5$) and four scans were obtained per sample.

2.5. Ellmans assay

The Ellmans assay was employed as outlined by Qie et al. [34] to determine the total thiol content of the HA-SH sample after lyophilisation, with some modifications. The Ellmans assay is a colorimetric assay which is based on the reaction between a thiol group and 5,5′-dithio-bis (2-nitrobenzoic acid) (DNTB), also known as Ellmans reagent. This reaction produces a TNB chromophore which has a λ_{max} of 412 nm [35]. The rate of formation of the TNB product is directly proportional to the concentration of thiol in the sample. The concentration of thiol in the HA-SH sample was determined from the linear equation or regression curve generated from a series of thiol standards, in this case cysteamine HCl. This method only detects free thiol in the samples and therefore in order to calculate the total thiol content, disulphide bonds formed in the

Table 1
Ratio of HA-MA to HA-SH (%wv).

Sample	HA-MA	HA-SH	Irgacure 2959
A	100	0	0.1
B	80	20	0.1
C	60	40	0.1
D	50	50	0.1
E	40	60	0.1
F	20	80	0.1
G	0	100	0.1

product required cleaving via 8 M urea during the Ellmans assay. Briefly, a set of cysteamine standards were prepared in reaction buffer (TGE buffer, pH 8.0, or TGE buffer with 8 M urea). A solution of 250 μl Ellmans (4 mg/ml in TGE buffer) in 12.5 ml reaction buffer was prepared and 250 μl was placed in each well of a 96 well plate. 25 μl of sample was added in triplicate, the plate was mixed and incubated for 15 min at room temperature. The absorbance was read at 412 nm and the concentration of thiol (mM) was interpolated from the standard curve. Total thiol content was obtained by adding the interpolated concentration (mM) of HA-SH in TGE buffer (free thiol) and HA-SH in 8 M Urea (bound thiol).

2.6. Nuclear magnetic resonance (NMR) spectroscopy

All spectra were recorded using a 500 MHz NMR spectrometer (Bruker Avance III). All spectra were recorded at 25 °C. Samples for NMR were dissolved in D_2O at ambient temperature to >10 mg/ 0.5 ml and diluted to ~1–2 mg/ml for ^{1}H NMR. ^{1}H-spectra with water suppression were recorded. For the purposes of purity checking and spectral assignment, ^{13}C/DEPT-90/DEPT-135/HH-CoSy/HSQC/HMBC spectra (not shown) were also obtained.

2.7. Reverse phase high performance liquid chromatography (RP-HPLC)

The degree of methacrylation was determined by RP-HPLC as previously described by [36]. In order to determine the effect of methacrylic anhydride starting concentration on the degree of substitution obtained, HA-MA was synthesized with different molar equivalents of methacrylic anhydride: 1×, 10× and 30×. These samples were then analysed as follows. HA-MA (15 mg) was dissolved in NaOH (aq. 0.02 M, 10 ml) and incubated at 37 °C for 30 min to enable hydrolysis of bound methacrylate groups from the polymer. A series of dilutions (1:2, 1:5 and 1:10) were prepared from this mixture in eluent and twenty microlitres in triplicate were then injected onto a column (XBridge BEH C18, 4.6 mm × 150 mm, 1.5 μm, 130 Å Waters Corp.). Analysis was performed on Nexera-*i* system (Shimadzu Corp.) equipped with a LC-2040 pump, LC-2040 autosampler and a PDA detector model SPD-M40. The elution was performed in isocratic mode at a flowrate of 1 ml min^{-1} with the mobile phase consisting of acetonitrile: water (15,85) adjusted to pH 2 with orthophosphoric acid. Peak areas from chromatograms obtained at 210 nm were analysed on LabSolutions software (Shimadzu Corp.) and subsequently used to quantify the degree of substitution of methacrylated hyaluronic acid.

2.8. Compression testing

Compression testing was carried out using a screw-driven mechanical testing machine (Lr10K, Lloyd Instruments, Bognor Regis, UK) fitted with a 2.5 kN load cell ($N = 5$). Samples were swollen to equilibrium in phosphate buffered saline (PBS) (pH 7.4) prior to testing and an unconfined compression was carried out at a speed of 1 mm/min using samples that were 20 mm in diameter and 1.8 mm in height as has been demonstrated in the literature [37]. A pre-load of 5 N was employed before compressing samples to 70 % strain [38]. Stress-strain curves were generated from which Young's modulus was calculated based on the linear portion of the graph. The stress at limit was calculated based on the load at the compressive limit of each sample.

2.9. Rheology

Rheological analysis was performed using an advanced rheometer AR1000 (TA instruments) fitted with a Peltier temperature control to investigate the comparative strength of samples. Samples were tested in quintuplicate, using individual samples, within 72 h of preparation using a 20 mm parallel steel plate with samples in the equilibrium swollen state. Amplitude sweeps were performed at a constant frequency of 1 rad/s with percentage strain ranging from 0.0001 % - 10 %. Dynamic frequency sweeps were performed at a constant strain of 0.01 % (linear viscoelastic region) with frequency ranging from 0.01 to 100 rad/s. Temperature ramps were performed between 4 and 37 °C in 2 °C increments with a soak time of 30 s. Prior to testing, samples were cut using a steel bore to 20 mm and blotted free of liquid using filter paper to minimise slippage. The compression load was constrained to 5 ± 0.2 N during testing and the mean ± SD of the storage and loss modulus under dynamic conditions were reported.

2.10. Swelling tests

The swelling behaviour of samples was analysed by rehydrating samples with a diameter of 25 mm and height of 1.8 mm to equilibrium in PBS (pH 7.4) and measuring the change in weight as a function of dry weight. The weight after photopolymerisation was recorded in quintuplicate before placing each individual sample in 10 ml PBS buffer. Once equilibrium swelling was reached (approximately 48 h), swollen weight (W_s) was recorded before vacuum drying the samples at 25 °C. The percentage swelling of the samples was calculated using the Eq. (1):

$$\text{Swelling } (\%) = \left(\frac{W_s - W_d}{W_d}\right) \times 100 \quad (1)$$

where W_s and W_d refer to the hydrogel in the equilibrium swollen state and dried state respectively.

The gel fraction of the hydrogels was measured by vacuum drying the hydrogel samples after photopolymerisation (W_d) before swelling to equilibrium in PBS (pH 7.4) (W_s) and finally, re-drying the samples using the vacuum oven (W_{redry}). Eq. (2) below was used to calculate the gel fraction of the hydrogels:

$$\text{Gel Fraction} = \left(\frac{W_{Redry}}{W_d}\right) \times 100 \quad (2)$$

2.11. Degradation tests

2.11.1. In vitro degradability

The degradability of hydrogel samples in physiological buffer was analysed by placing samples of 20 mm diameter in a 6 well tissue culture plate in quintuplicate and submerging each hydrogel in PBS (pH 7.4). Weights were recorded every 24 h for 7 days.

2.11.2. Accelerated degradation study

Hydrogel samples of 20 mm diameter were placed in a 6 well plate in quintuplicate. Hydrogel samples were submerged in either 5 mM or 5 M NaOH and weights were recorded every 24 h for 7 days.

2.11.3. Hyaluronidase degradation study

24 well tissue culture plates were coated in either HA, HA-SH or HA-MA respectively by dissolving the HA or HA derivative in 0.1 mg/ml PDL and coating each well in this solution. After washing and drying the coated plates, a control solution (PBS) or 0.4–1 IU hyaluronidase was added to each well and aliquots were collected every 15 min to monitor the degradation of HA. The aliquots were collected by removing the entire solution from the well to microtubes, maintaining replicates, before replacing with fresh control solution or enzyme. These samples (in triplicate) were then put through a carbazole assay ($N = 2$) to quantify the uronic acid present in each sample. The carbazole assay is a colorimetric method of quantification of uronic acid which is a component of hyaluronic acid [39]. In this way, this assay can measure the amount of HA in a sample. In this study, the carbazole assay was used to quantify the amount of HA degraded from the coating via hyaluronidase in order to evaluate the differences in degradability between unmodified, thiolated and methacrylated HA.

3. Results

3.1. Preparation of HA derivatives

3.1.1. Cysteamine modified hyaluronic acid

Previous research has demonstrated the efficacy of modifying HA with thiols such as *N*-acetyl Cysteine (NAC) for the aim of drug conjugation [40]. Based on the studies of these scientists, it was chosen to use cysteamine due to its simpler structure, thus avoiding the steric hindrance observed with NAC. In addition, various carbodiimide and catalyst systems were evaluated to determine which system produced the most reproducible and reliable modification by advancing the reaction prior to the synthesis of stable *N*-acyl urea. In order to make cysteamine-modified HA (HA-SH), the carboxyl group was activated with EDC and DMAP, followed by a reaction with cysteamine hydrochloride. This reaction mechanism is illustrated in Fig. 2 above. EDC was selected because to its greater solubility in water. This solution was dialyzed thoroughly prior to lyophilisation. The product dried into a fluffy, white, sponge-like substance, and the yield was consistently 90 ± 5 %. Modification was confirmed by ^{1}H NMR analysis and the Ellmans assay. Fig. 3a. shows the ^{1}H NMR spectrum of thiolated vs native HA with water suppression. The methylene protons of cysteamine can be observed at 2.9 ppm and 3.04 ppm as seen in the HA-SH spectrum below. Quantification of thiolation was conducted via the integration of the peaks relative to the *N*-acetyl peak of HA, which is labelled as (1) in the Fig. 3(a) below. The Ellmans assay detects both free and bound thiol groups colorimetrically and the results are depicted in Fig. 3b. Fig. 3b. illustrates the linear relationship with a coefficient of determination of 0.99 for both standard curves of standards in both reaction buffer and 8 M urea from which unknowns were measured. In reaction buffer, the concentration of free thiol was calculated to be 0.29 mM, and after treatment with 8 M urea the concentration of bound thiol was calculated to be 0.225 mM. Therefore, the total thiol content of the sample was determined to be 0.515 mM. The calculated degree of modification (MoD) was determined to be approximately 27.7 % from the NMR data obtained and approximately 22 % from the Ellmans assay. These values are above the 20 % modification degree mentioned earlier and therefore risks alteration of CD44 functionality. However, as the exact implications of altering CD44 functionality is not yet known, samples with a modification degree of between 20 and 30 % were used for testing.

3.1.2. Methacrylate modified hyaluronic acid

HA-MA was initially produced as per literature [36] which states a 20-fold molar excess of methacrylic anhydride should be used. It was established that this resulted in too high of a degree of substitution for this purpose and therefore, a 10-fold molar excess of methacrylic anhydride was used in subsequent reactions. This resulted in a product which was approximately 20 % modified as measured by ^{1}H NMR shown in Fig. 4(b). Three separate batches were tested which resulted in modification degrees of 20 % +/− 9 % as determined via ^{1}H NMR, RP-HPLC and ATR-FTIR. The correlation between ^{1}H NMR and RP-HPLC proved to be very robust with RP-HPLC quantifying the degree of modification to be 25 % +/− 3 % and ^{1}H NMR calculated at 20 % +/− 9 %, this was not surprising as ^{1}H NMR lacks the sensitivity of RP-HPLC. Fig. 4(a) below shows a comparison of unmodified HA (HA), thiolated HA (HA-SH) and methacrylated HA (HA-MA). The presence of a peak at 1712 cm^{-1} arises from the methacrylic ester carbonyl vibration, confirming successful methacrylation. Fig. 4(b) shows the presence of vinyl protons at ~5.9 and 6.1 ppm which arise from the methacrylate group and were used to measure the degree of modification relative to the integration of the *N*-acetyl peak at ~2 ppm.

RP-HPLC was used to confirm the degree of substitution obtained via NMR analysis. Fig. 5 shows the 3D chromatograms (a) of diluted samples of unmodified HA (i), 1× HA-MA (ii), 10× HA-MA (iii) and 30× HA-MA (iv) where the fold number refers to the molar equivalents used during the modification process.

Also shown in Fig. 5 is the chromatogram overlays of samples (b) and the calibration curve of methacrylic acid samples (c) from which the degree of substitution of HA-MA was calculated. Due to increased reactivity, as a result of lower steric hindrance, the primary alcohol at C6 of the *N*-acetylglucosamine moiety undergoes modification chemoselectively. It was found that using a 1 M equivalent of methacrylic anhydride resulted in 6 ± 0.9 % of primary hydroxyls modified, a 10-fold molar excess of methacrylic anhydride resulted in 25 ± 3 % and a

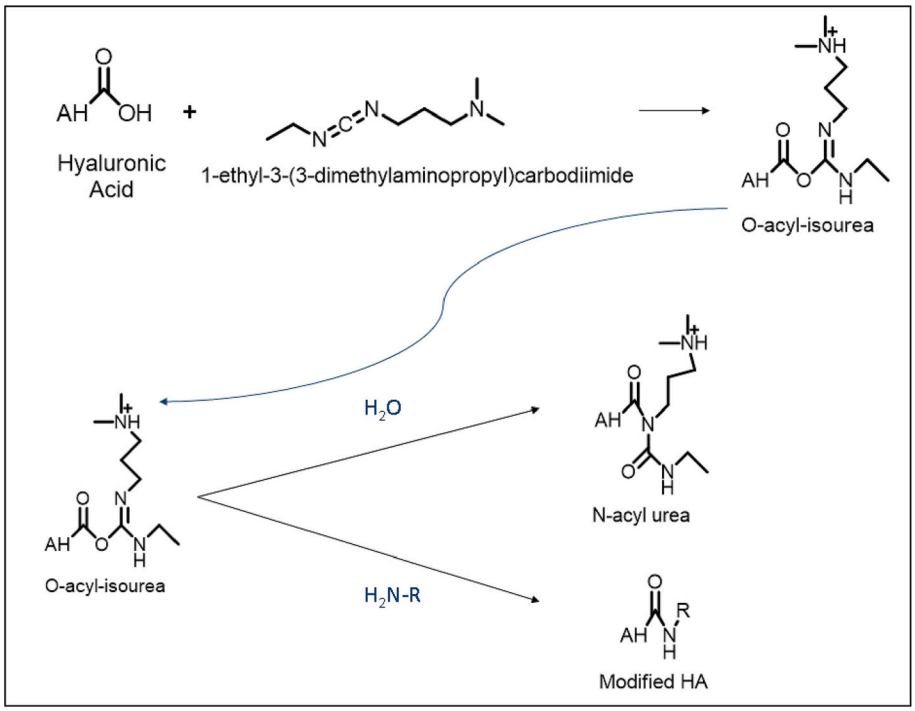

Fig. 2. Reaction scheme for thiolation of HA via amidation [4]. Functional group "R" to depict thiolation.

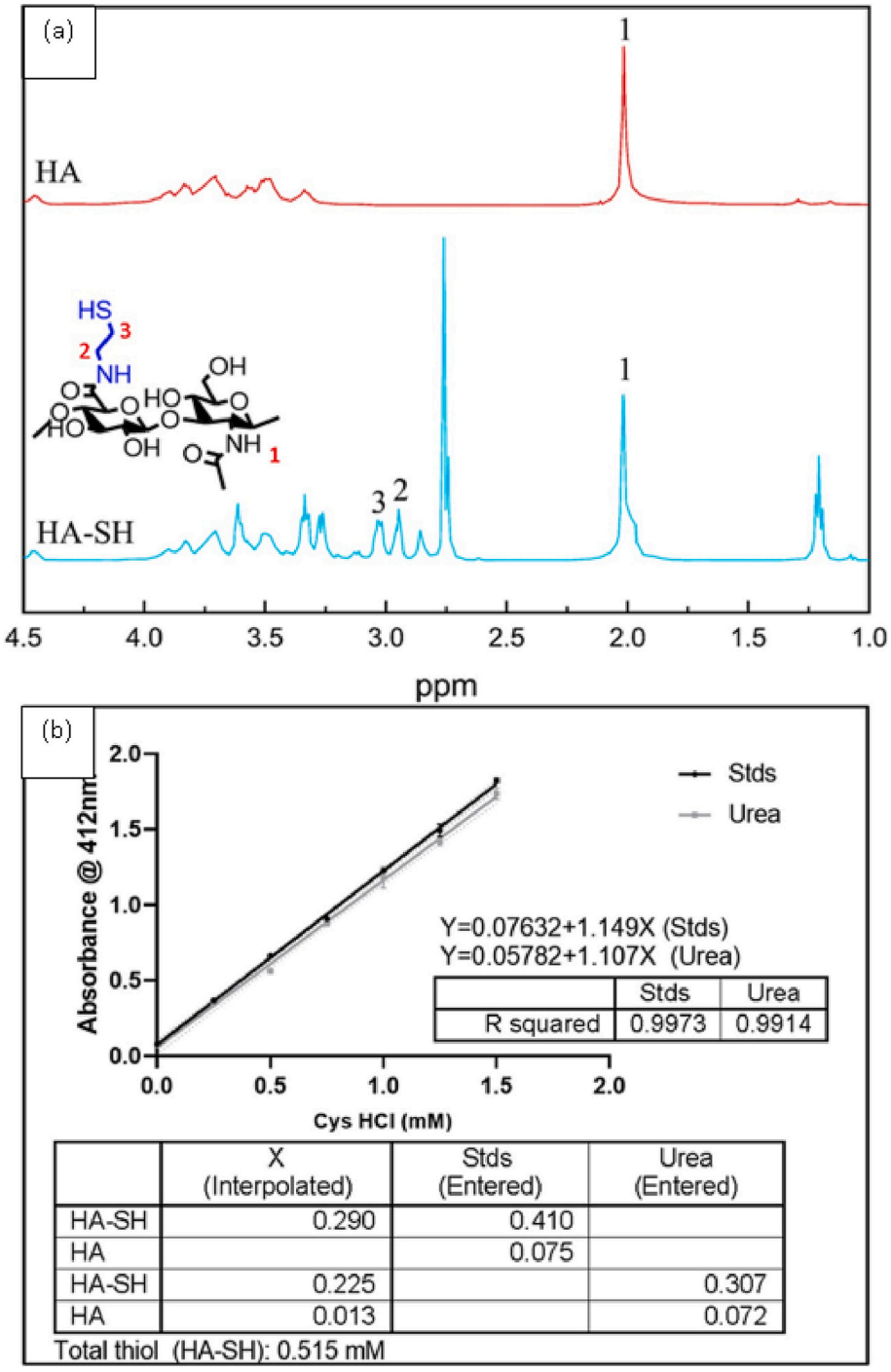

	X (Interpolated)	Stds (Entered)	Urea (Entered)
HA-SH	0.290	0.410	
HA		0.075	
HA-SH	0.225		0.307
HA	0.013		0.072

Fig. 3. (a) ^{1}H NMR comparison of unmodified HA (HA) vs cysteamine modified HA (HA-SH). The methylene protons of cysteamine can be observed at ~2.9 ppm and 3.04 ppm; (b) Ellmans assay determination of total thiol content in HA-SH.

30-fold excess of methacrylic anhydride resulted in 124 ± 10 % of primary hydroxyls modified. The degree of substitution (DS) of HAMA was calculated using Eq. (3) below as adapted from [41]:

$$DS = \frac{MW_{HAU} \times m_{MA}}{MW_{MA} - m_{net} \times m_{MA}} \quad (3)$$

where:

MW_{HAU}: Molecular weight of anhydrodisaccharide unit of hyaluronic acid.

m_{MA}: Mass of methacrylic acid in sample of modified hyaluronic acid.

MW_{MA}: Molecular weight of methacrylic acid.

m_{net}: Net increase in mass of anhydrodisaccharide unit for each methacrylate group substituted.

These results agreed with the degree of modification calculated via NMR and on this basis, a 10-fold excess of methacrylic anhydride was used for subsequent modifications.

3.1.3. Cross-linking of HA derivatives

Various blends of HA derivatives, as outlined in Table 1, were photopolymerised after 10 min of UV exposure. The reaction scheme for UV photopolymerisation of thiolated and methacrylated HA is outlined in Fig. 6. below. This timing was deemed sufficient for complete

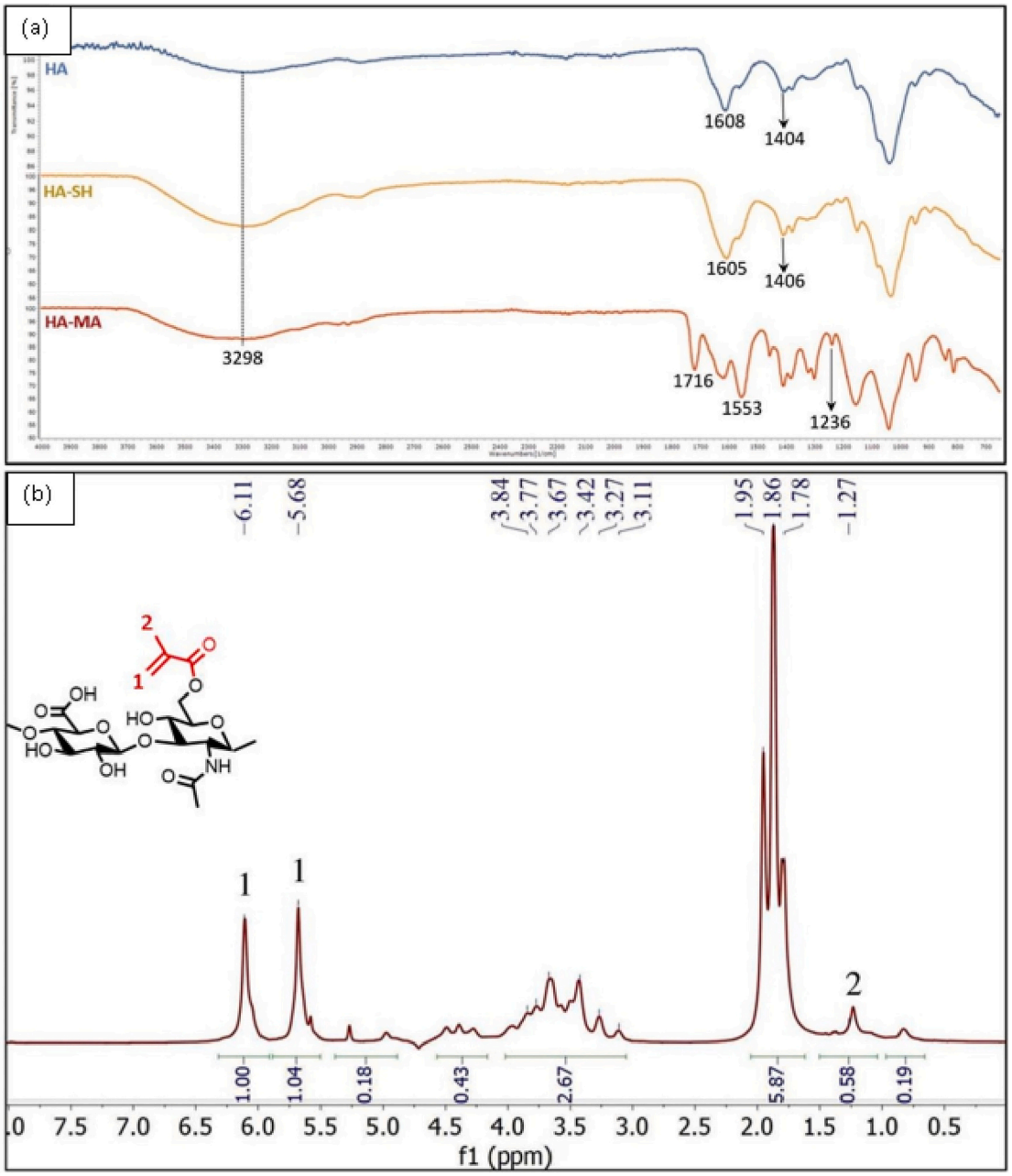

Fig. 4. (a) FTIR spectra (top) of unmodified HA (HA), Thiolated HA (HA-SH) and methacrylated HA (HA-MA). (b) The ^{1}H NMR spectrum (bottom) shows the presence of the vinyl protons of methacrylate at approximately 5.9 ppm and 6.1 ppm.

polymerisation of samples following several optimisation experiments not shown within this manuscript. Samples F and G were found to insufficiently cross-link within this period of time, and therefore were excluded from further testing. Insufficient cross-linking was determined by the lack of gel formation after the initial 10 min of UV-curing time. A further trial of 30 min UV-exposure was conducted to assess whether prolonged exposure to UV would enable cross-linking to occur but on removal from the chamber, no gel solids were observed in the silicone mould. As HA remained in the viscous liquid state at these concentrations, they were deemed insufficiently cross-linked. This insufficient polymerisation is thought to be due to insufficient methacrylate moieties for the thiol to react across in an 80MA: 20SH ratio. Polymerisation occurs in this process through free radical chain polymerisation in which the production of free radicals via the photo-initiator and UV light initiates a polymerisation reaction between the thiol group and methacrylate moiety. 100%wv HA-SH did not photo-polymerise under UV due to the absence of the methacrylate moiety but the formation of disulphide bonds occurred when the sample was allowed to sit at room temperature for 30 min which produced a polymer film (not shown). Following removal from the UV chamber, the hydrogels were rinsed with deionised water and blotted free of solution before storage protected from light. All hydrogels were used within 72 h of photopolymerisation.

3.2. Biocompatibility of HA derivatives

The biocompatibility of HA derivatives post-modification (not cross-linked) was evaluated using the resazaurin reduction assay and neutral red uptake assay as shown in Fig. 7. below. 24 well tissue culture plates were coated in HA or HA derivatives dissolved in 0.1 mg/ml PDL to ensure a homogenous coating. Cells were seeded and grown overnight on the coated surface before the addition of either resazaurin or neutral

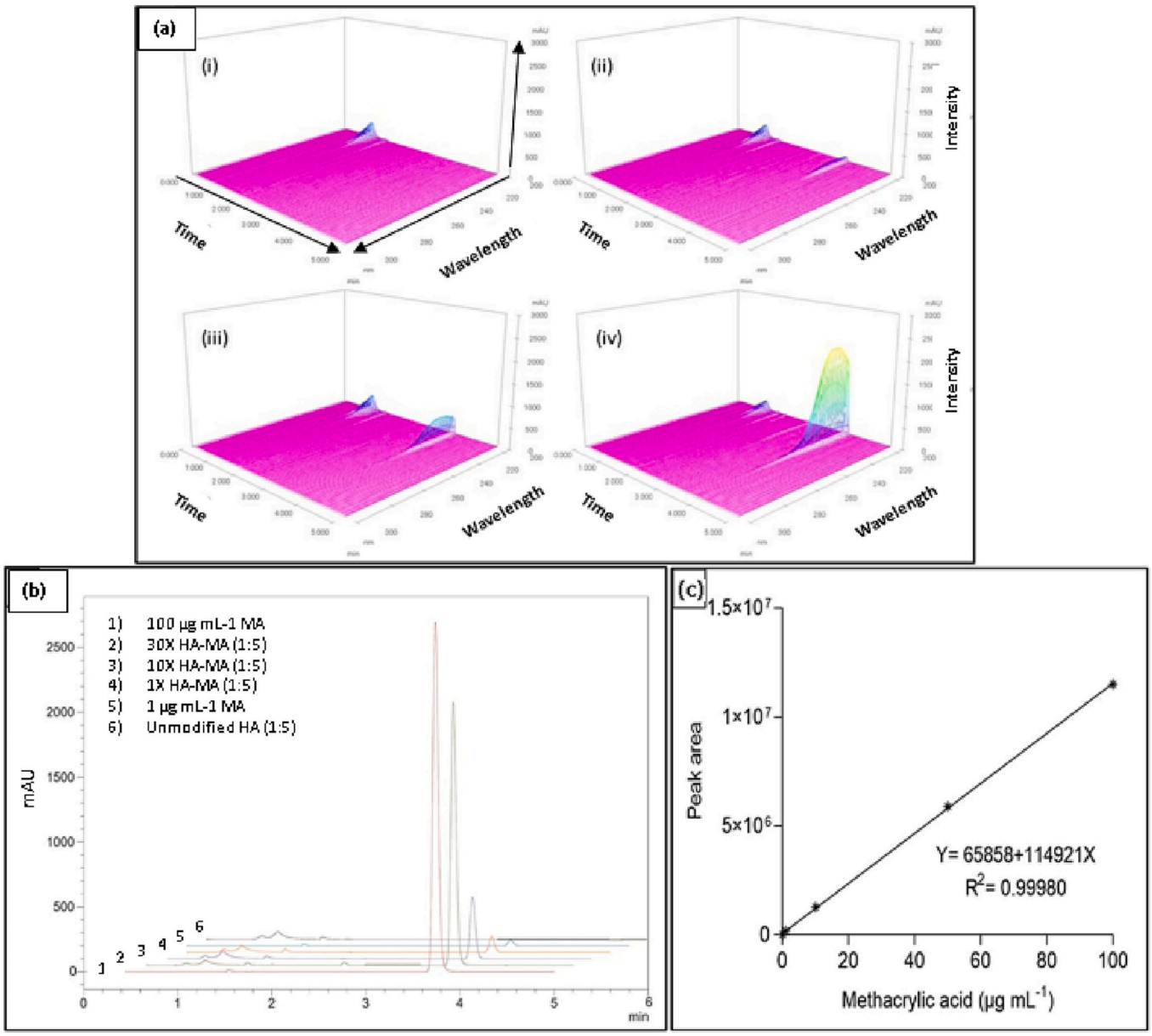

Fig. 5. (a) 3D chromatograms of 1:5 diluted samples of (i) HA, (ii) 1× HA-MA, (iii) 10× HA-MA and (iv) 30× HA-MA. (b) Chromatogram overlay of samples at 210 nm. (c) Calibration curve of methacrylic acid standards (0.05–100 µg/ ml).

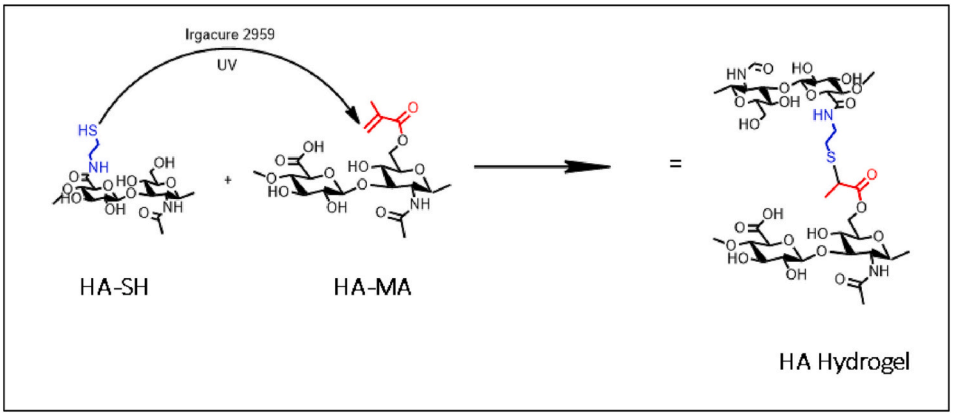

Fig. 6. UV photopolymerisation of HA-SH and HA-MA

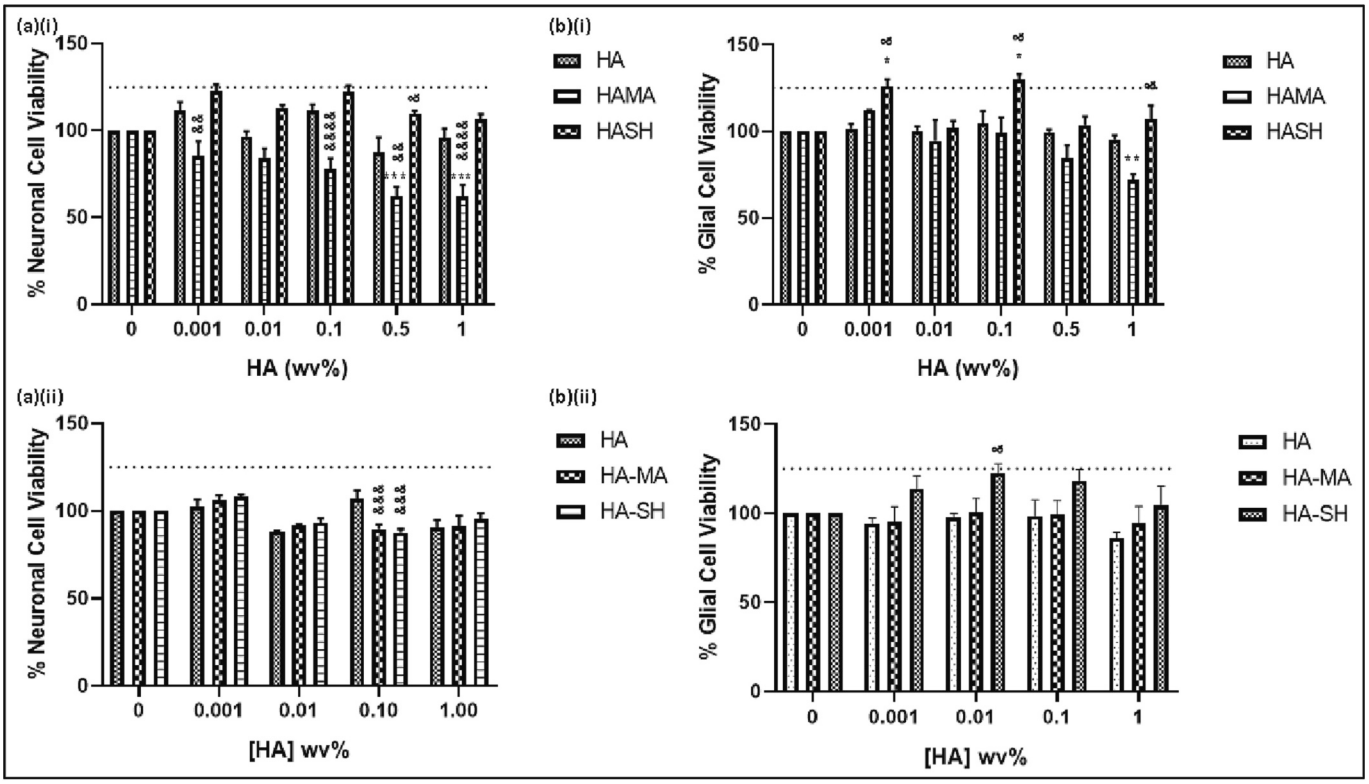

Fig. 7. Cell viability of neuronal (a) and glial (b) cells after 24-h exposure to native HA or the modified derivatives. Assays were conducted using the resazaurin reduction assay (i) and neutral red uptake assay (ii). Data represents mean ± SEM of three independent experiments, conducted in triplicate. $^{*}P < 0.05$, $^{**}P < 0.01$, $^{***}P < 0.001$ vs control (0%wv HA); $^{\&}P < 0.05$, $^{\&\&}P < 0.01$, $^{\&\&\&}P < 0.001$ vs native HA equivalent when compared using two-way ANOVA with Tukey post-tests. HA control (0%wv) refers to 0.1 mg/ml PDL. (For interpretation of the references to colour in this figure legend, the reader is referred to the web version of this article.)

red. The resazaurin assay works on the basis of the conversion of non-fluorescent resazaurin to resorufin, a fluorescent compound, via cell metabolism which is dependent on intracellular oxidoreductases [42]. The neutral red uptake assay, however, relies upon the inhibition of lysosomal uptake of the neutral red dye to determine cell viability as only live cells internalise the dye [43]. By utilising a battery approach, a more objective stance is taken by looking at both metabolic and non-metabolic cell viability assays. The assays were performed as detailed in the literature [44,45]. As previously noted, HA lacks the sites necessary for cellular adhesion and therefore can be difficult to evaluate through in-vitro assays. However, through modification, HA can facilitate increased attachment as shown by the increase in cell viability observed in the presence of thiolated HA (HA-SH) in glial cells when compared to control (0 % HA) ($^{*}P < 0.05$, $^{**}P < 0.01$) and vs native or unmodified HA at equivalent concentrations ($^{\&}P < 0.05$) (Fig. 6(b)(i)). This is in contrast to the decrease in compressive strength and modulus noted in Section 3.4 with increasing HA-SH concentration, however, the hydrogels tested were not cell laden which can impart increased mechanical properties to a hydrogel. In addition, biocompatibility testing was performed on HA derivatives in isolation- that is, powder form dissolved in PDL rather than cross-linked in hydrogel form.

Decreased cell viability was observed in neuronal cells exposed to methacrylated HA ($^{***}P < 0.001$ vs control) when assayed with resazaurin but this result was not significant when assayed using neutral red. Glial cells also displayed decreased viability when exposed to 1%wv HA-MA when assayed with resazurin but similarly, this significance was not replicated by the neutral red uptake assay. Increased cell viability ($^{*}P <$ 0.05 vs control) was observed in glial cells exposed to thiolated HA (HA-SH) vs control when assayed using resazaurin but this result was not significant via neutral red although a similar trend was observed. Glial cells showed increased viability after exposure to HA-SH vs native HA ($^{\&}P < 0.05$) at various concentrations when assayed using both resazaurin and neutral red uptake. Differences in the significance between assays is due to differences in sensitivity and selectivity between assay modes and highlights the requirement for a battery approach in cytotoxicity testing. In all cases, the control referred to PDL coating without HA.

3.3. ATR-FTIR of photo-polymerised samples

Post-polymerisation, samples for characterisation were dried in a vacuum oven to rid the samples of excess water. FTIR analysis of photo-cured samples revealed a loss of peaks at 1553 and 1236 cm^{-1} (highlighted in Fig. 4 above) which arise from the C═C stretching and C—O stretching of methacrylate which can be seen in Fig. 8. below. This confirms polymerisation has taken place. Generally, the broad absorption band at 3700–3200 cm^{-1} corresponds to the vibrations from O—H stretching.

The thiol bearing HA shows little change in the FTIR however, the signal resulting from the thiol SH is likely broadened by the polymeric nature of the sample and while the C—S is in the fingerprint region (400–1500 cm^{-1}).

3.4. Compression testing

Compressive strength of a polymer dictates the force a hydrogel can withstand which is an important parameter for the design of medical devices or many other bioengineering applications. The ideal scenario would present a polymer blend with sufficient strength to withstand compressive forces in vivo while still retaining the elasticity necessary to facilitate regeneration of tissues. Fig. 9. below illustrates the compressive strength at limit and the Young's modulus for each hydrogel. The compressive strength of each sample decreased with increasing concentration of thiols showing the decrease in stiffness of all hydrogels

Fig. 8. ATR-FTIR spectra of HA-MA: HA-SH hydrogels of varying concentration.

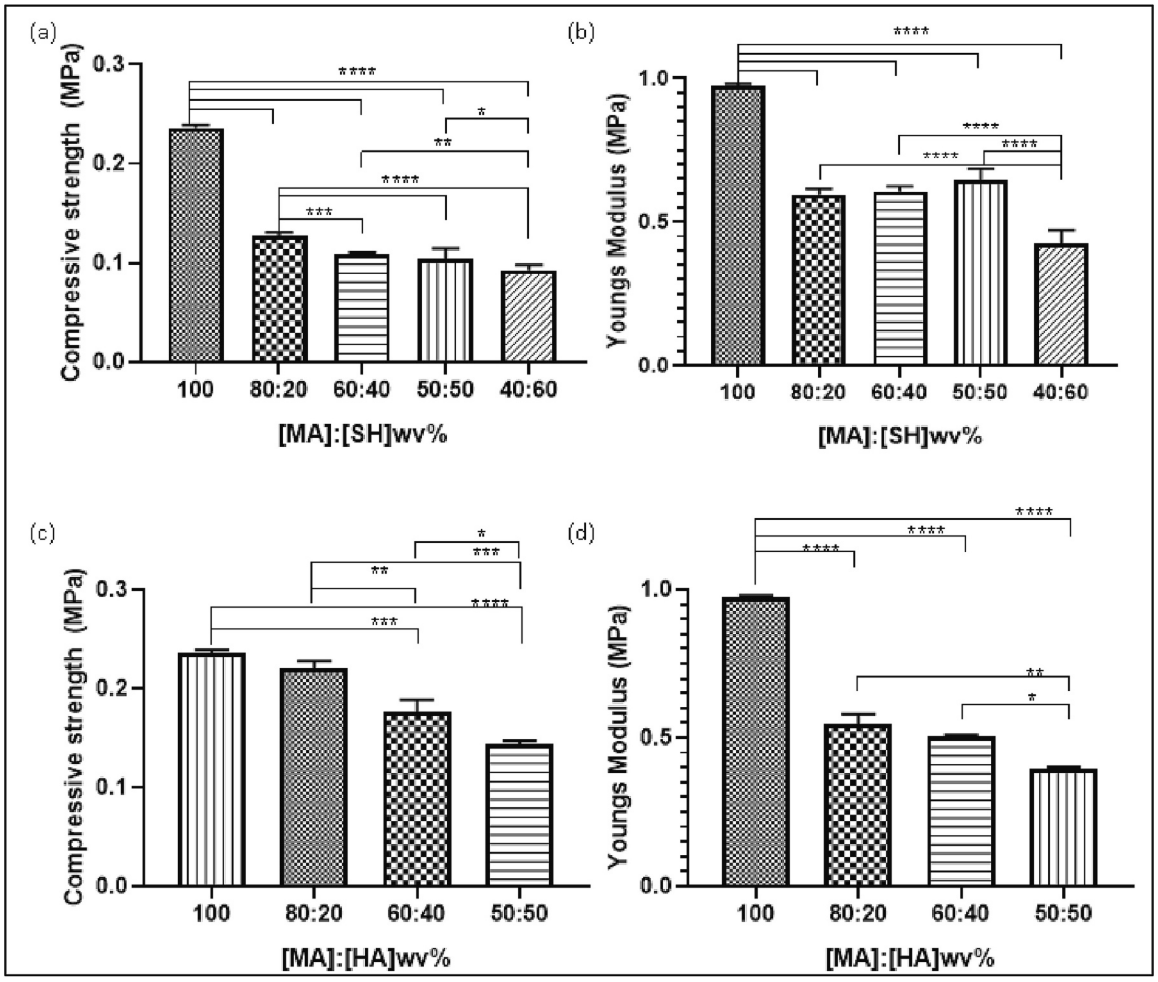

Fig. 9. The compressive properties of HA derivative hydrogels showing (a/c) the compressive strength of HA-MA: HA-SH blends and HA-MA: unmodified HA control blends and (b/d) the Young's modulus of same. Data is the mean ± SEM of 5 independent experiments, conducted in triplicate. (*$P < 0.05$, **$P < 0.01$, ***$P < 0.001$, ****$P < 0.0001$ when comparing conditions using one-way ANOVA with Tukey post-tests).

proportional to thiol concentration. The Young's modulus, which is the gradient of the line in a stress strain plot, remained relatively constant across the 80:20, 60:40 and 50:50 [MA]: [SH] HA blends.

Increases in thiol concentration proportionally increases the elasticity of a hydrogel as is made evident by Fig. 9 (a-b) which clearly shows a deficit in compressive strength relative to thiol concentration. This could be due to the reduced bond strength observed with increased thiol concentration as has been reported in literature when cross-linking with methacrylate (Sara [46]). Interestingly, this decrease in compressive strength is greater with the introduction of thiol than the control (c-d) which was HA-MA in various ratios with unmodified HA. The unmodified HA should not crosslink and therefore the sample should be cross-linked HA-MA with unmodified HA molecules existing within the cross-linked network. In all cases, 100 % HA-MA had a compressive strength of approximately 0.24 MPa, however, an introduction of 20 % thiol reduced the compressive strength observed to approximately 0.12 MPa. Conversely, replacing the thiol content with unmodified HA resulted in a reduction of compressive strength of 0.02 MPa which is a difference of 0.1 MPa from the introduction of thiol. The Young's modulus shown in (b) and (d) highlight the greater elasticity in the matrix of thiol containing hydrogels as figure (d) shows a proportional decrease to the lower concentrations of methacrylate in the matrix,

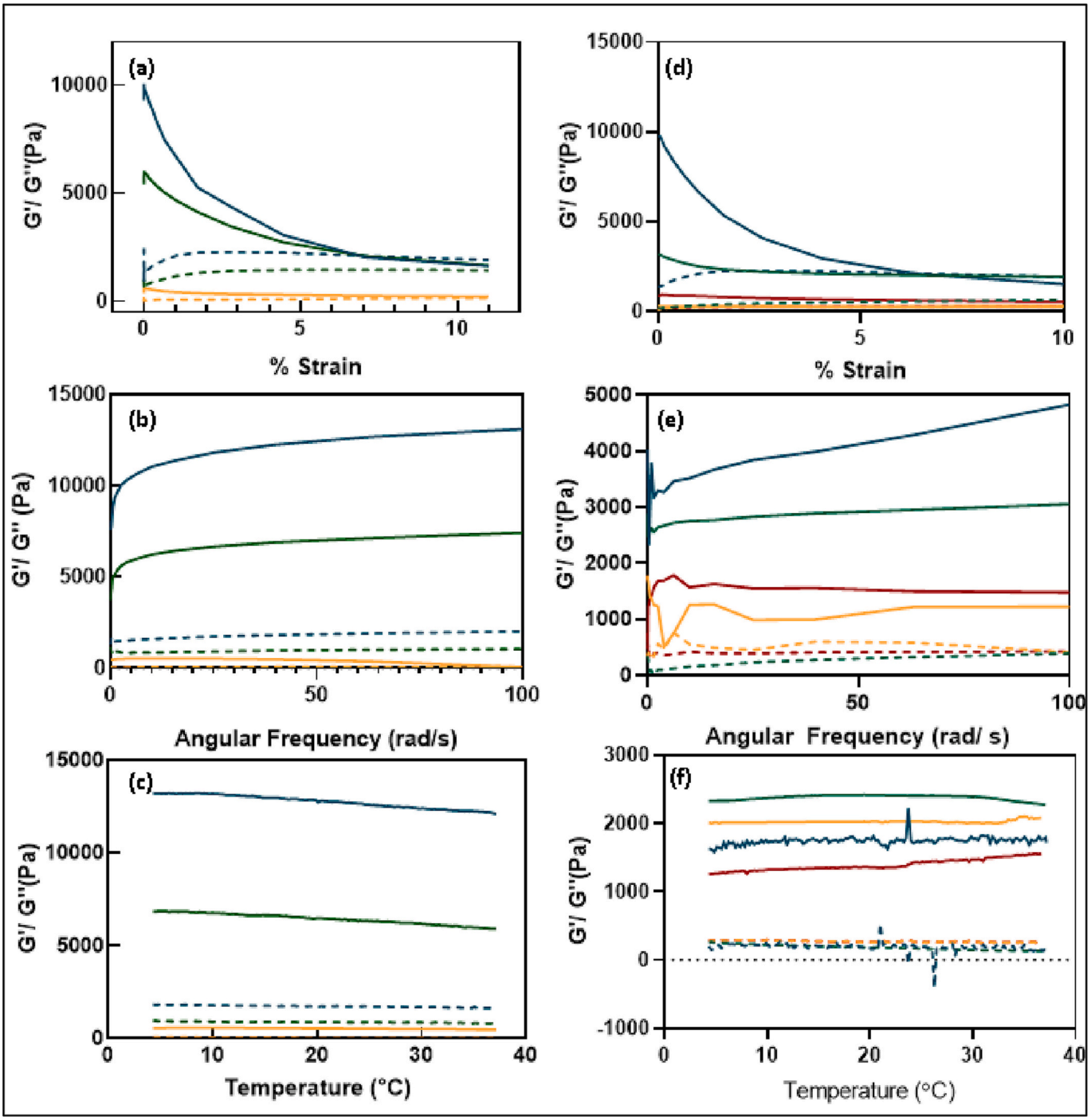

Fig. 10. (a-c) Rheological characterisation of HA-MA derivative blends with deionised water. (d-f) Rheological characterisation of HA-MA and unmodified HA blends. (a/d) Amplitude sweep, (b/e) Frequency sweep and (c/f) Temperature ramp of HA derivative hydrogels.

whereas (b) shows a steady Young's modulus across concentrations up to 40%wv methacrylate where a stark decrease in observed. In order to perfect the balance between a flexible hydrogel and a hydrogel with sufficient compressive strength for specific bioengineering applications, the ratio of thiol to methacrylate in the HA hydrogel could be fine-tuned or alternatively a *co*-polymer could be used with higher compressive strength as noted by [47].

3.5. Rheology

Rheological characterisation of the hydrogels is shown below in Figs. 10 and 11. The storage modulus of a hydrogel shows the ability of a hydrogel to store strain energy and is directly related to the cross-linking density of a polymer. Fig. 11 (g-i) below shows that as the thiol concentration increases, so too does the storage modulus and in turn, the degree of crosslinking, up to a ratio of 50:50. This is due to the formation of thiolene bonds between the methacrylate and thiols. This is especially evident when comparing Fig. 10(a-f) with Fig. 11 (g-i). Panels (a-c) show samples of HA-MA hydrogels prepared with deionised water in place of thiol, whereas in samples (d-f), samples were prepared as a blend of HA-MA and unmodified HA in various ratios. This was done in order to have a suitable control to compare the thiolene methacrylate hydrogels as confirmation of the presence of thiolene bonds. It is evident when comparing these graphs that the thiol imparted better mechanical properties on the hydrogels than deionised water or unmodified HA, i.e. in Fig. 10(a), 60:40 HA-MA: deionised water had a storage modulus of <1000 Pa, whereas in Fig. 11(g) 60: 40 HA-MA: HA-SH had a storage modulus of almost 50,000 Pa. This is indicative of the presence of thiolene bonds resulting in a more highly elastic hydrogel. All samples remained stable across a temperature range of 4–37 °C showing that the storage modulus of the material would not be affected through storage or physiological temperature exposure. This is an important

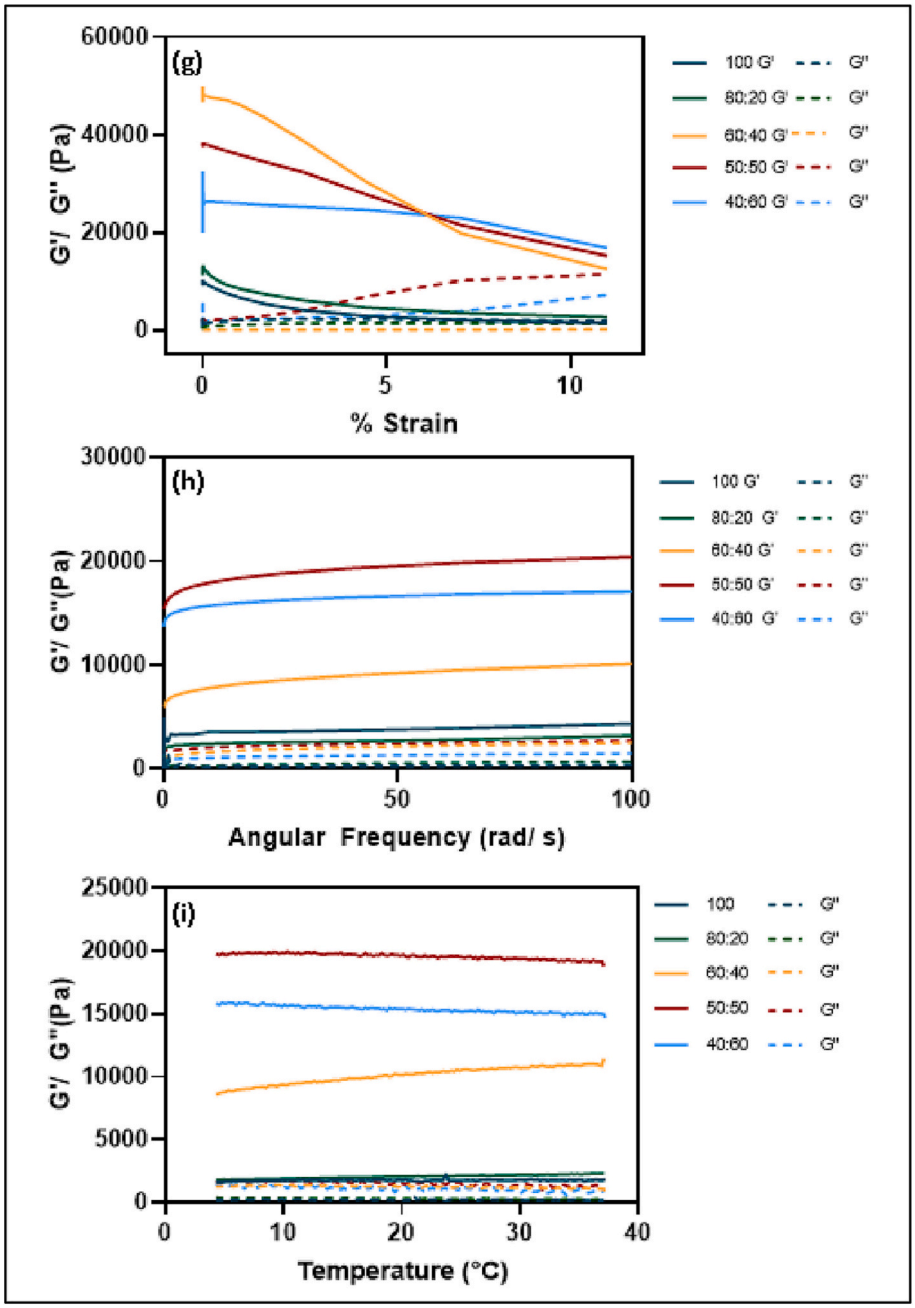

Fig. 11. (g-i) Rheological characterisation of HA-MA and HA-SH. (g) Amplitude sweep, (h) Frequency sweep and (i) Temperature ramp of HA derivative hydrogels.

characteristic for a potential medical device formulation. Also shown in Fig. 10 and Fig. 11 is the evolution of the viscous or dissipative (G") modulus as a function of strain, frequency and temperature. As expected, in all cases, hydrogels displayed a gel-type mechanical spectra (G' > G"). However, a cross-over modulus was observed in (a) at a strain of approximately 7.8 % and (d) at approximately 5.5 % strain in the case of 100%wv HA-MA and 80%wv HA-MA where the hydrogel began to show more viscous like characteristics as the % strain increased.

Typically, in viscoelastic samples it would be expected that the storage moduli of samples would be equal to the Young's moduli of samples, however, when comparing Fig. 9 with Fig. 10 and Fig. 11, the opposite is true in terms of this material. 100%wv HA-MA hydrogels showed a higher Young's modulus than thiol containing samples in compression testing but performed worse in rheological analysis. This may be due to the increased elasticity imparted by the thiolene bonds due to the decrease in bond strength in the thiolene network versus the methacrylate network.

3.6. Swelling tests

The degree to which a hydrogel swells is due to how tightly networked the polymer matrix is after photopolymerisation [49]. Significant increase in weight due to swelling would indicate a greater amount of space between polymer chains, as would be expected with high molecular weight molecules such as HA. The degree of swelling of a medical device must be carefully monitored and should be within expected and defined parameters, therefore it is a vital investigation. The mean swelling ratio (Q) shown in Fig. 12 increased with increasing thiol content in the hydrogels. This is in contrast to what was expected as increased cross-linking density in hydrogels would typically result in less swelling. However, this was non-significant and the slight increase in swelling could be attributed to the enhanced degradation observed in thiolene hydrogels as illustrated in Fig. 13 below. The gel fraction of hydrogels initially decreased when comparing 100%wv HA-MA to the 80: 20%wv HA-Ma: HA-SH blend, however, this was non-significant and the gel fraction remained consistent across all other concentrations, further confirming the presence of cross-linked network between the HA-MA and HA-SH components.

No significant differences were observed when comparing the Q ratio between HA-MA: HA-SH hydrogels and the control HA-MA: HA hydrogels. However, in both cases an increase in swelling was observed across concentrations. This swelling was not significant when comparing across concentration. The control hydrogels (HA-MA:HA)showed decreases in the gel fraction % proportional to the decrease in HA-MA concentration. This is in contrast to the HA-MA: HA-SH hydrogels which showed an initial decrease in gel fraction before stabilising across the concentration ranges 80:20 to 40:60%wv.

3.7. Degradation tests

HA is readily degraded by endogenous enzymes known as hyaluronidases in the body. In order to replicate the conditions of degradation in a variety of conditions, hydrogels or polymer blends were exposed to various conditions such as pH 7.4 buffer (physiological pH), 5 mM NaOH (mildly accelerated), 5 M NaOH (accelerated) and pH 7.4 buffer containing the hyaluronidase enzyme. The degradation of HA in hydrogels was assessed under physiological conditions (pH 7.4) and accelerated degradation (5 mM/ 5 M NaOH). In order to evaluate the degradation of HA and HA derivatives in the presence of hyaluronidase (0.4–10 IU), 24 well tissue culture plates were coated in HA or HA derivative dissolved in 0.1 mg/ml PDL. Dissolution in PDL was to provide a homogenous coating in the base of the well. Once coated, 0.4–1 IU hyaluronidase was added to the well and samples were removed every 15 min to monitor the enzymatic activity. The concentration of uronic acid at each time point was calculated via the carbazole assay. The carbazole assay is a method used to quantify the amount of HA colorimetrically via uronic acid [50]. The theory behind this assay design was that as the enzyme cleaved HA from the coating on the bottom of the plates, uronic acid would be released into the media and could then be quantified. The amount of uronic acid detected in each sample would reflect the degree to which each HA sample was degraded, or released from the plate coating, by the enzyme in that specific time period. In this manner, it would be clear to see the effect that modification has on the ability of hyaluronidase to cleave HA. After samples were collected, they were placed at 4 °C until assayed.

In all cases, the addition of thiols resulted in a decrease in resistance to degradation as shown in Fig. 13. In pH 7.4, there were significant differences between the rates of degradation when comparing HA-MA and the MA-SH blend at day 2 and day 3 (****$P < 0.0001$ and **$P < 0.01$ respectively), however, after this point no significant difference was observed. Similar observations were made with 5 mM NaOH and 5 M NaOH. When comparing native HA to the HA derivatives in Fig. 13 (d), it was found that methacrylation imparts a greater resistance to hyaluronidase when compared with native HA at the 30 min time point (**$P < 0.01$). This finding is also evident in the images of HA-MA hydrogels vs 50 % HA-MA: HA-SH hydrogels taken at days 1, 3 and 7 as shown in Fig. 14 below where it can be seen that a higher methacrylate concentration imparts a greater resistance to degradation. By day 7, only the HA-MA hydrogel in 5 M NaOH had completely degraded, whereas all 50 % MA-SH hydrogels had degraded completely.

These findings imply that by balancing the ratio of methacrylate to thiol, degradation can be tailored based on the application of the product and the residence time required.

However, as has been illustrated in Fig. 7, HA-MA is not without limitations as it does display greater toxicity in neuronal and glial cell lines than HA-SH or native HA. Therefore, depending on the intended

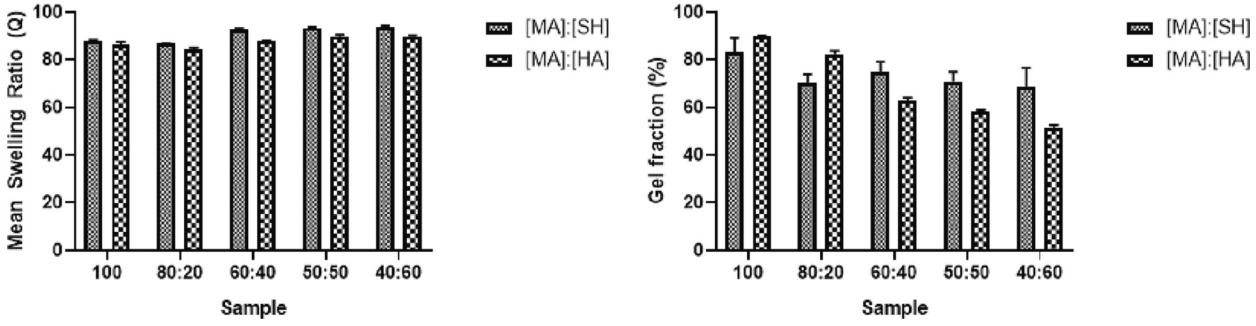

Fig. 12. Comparison of the swelling characteristics of HA-MA hydrogels with increasing thiol concentration with HA-MA: HA controls. Data shown is the mean ± SEM of 5 independent experiments, conducted in triplicate. No significance ($P > 0.05$) was detected between concentrations when comparing HA hydrogels with various ratios of methacrylate: thiol using one-way ANOVA with Tukey post-tests. No significance ($P > 0.05$) was detected when comparing [MA]: [SH] vs [MA]: [HA] using two-way ANOVA with Tukey posttests.

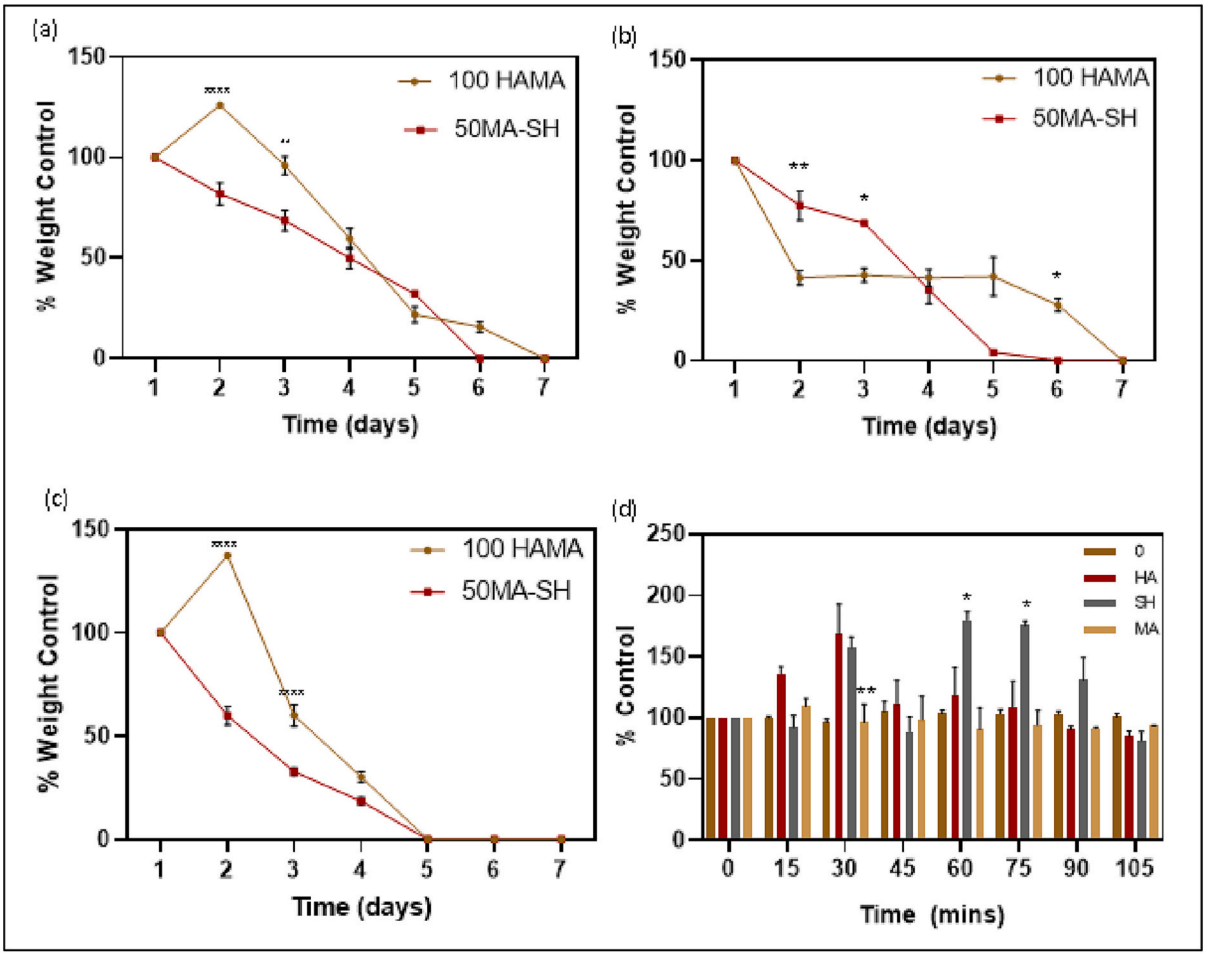

Fig. 13. Degradation of hydrogels of HA derivatives in pH 7.4 (a), 5 mM NaOH (pH 11.7) (b), 5 M NaOH (pH 13.7) (c) and hyaluronidase degradation of derivative powders (d). Data is the mean ± SEM of 2 independent experiments, performed in triplicate. *$P < 0.05$, **$P < 0.01$, ***$P < 0.001$, ****$P < 0.0001$ vs 100 HA-MA (a, b, c) or native HA equivalent (d) when compared using two-way ANOVA with Tukey post-tests.

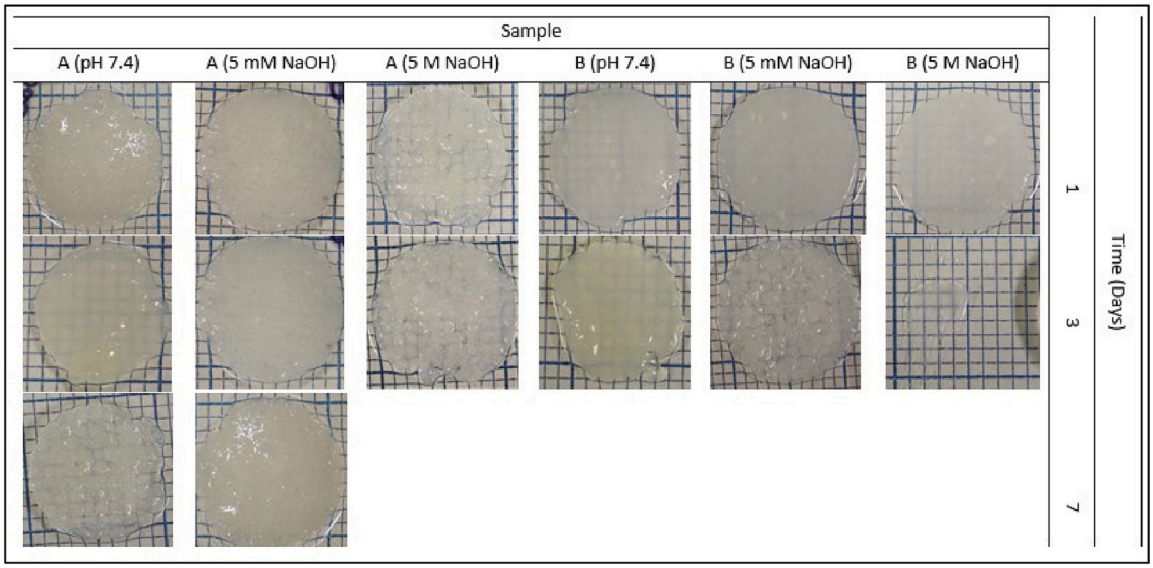

Fig. 14. HAMA (A) and 50 % MA-SH hydrogels (B) after exposure to pH 7.4, 5 mM NaOH or 5 M NaOH.

application within the human body, consideration would need to be given to the surrounding tissue viability/ health and the intended half-life of the polymer. It is necessary in all cases to balance the need for longevity of the polymer and resistance to endogenous degradation with the expected toxicity. This balance can be achieved by altering the ratio of thiolation and methacrylation dependant on the end application of

the polymeric construct.

4. Conclusion

Using click chemistry crosslinking, we have developed a novel biodegradable HA hydrogel. As demonstrated by rheology and biocompatibility studies, the addition of thiolated HA to methacrylated HA improved the degradation and biological properties of this hydrogel compared to methacrylated HA alone. This is evidenced by the increased storage modulus due to the increased elasticity relative to increasing thiol concentration. This elasticity was also observed in the compressive strength as a decrease in strength was observed proportional to thiol concentration. This is a factor which would need to be considered in bioengineering applications. Our research indicated that the HA derivatives could maintain cell viability in neuronal and glial cell lines and the hydrogels of these derivatives could successfully biodegrade in the body. However, a major limitation of this study was that cells were not tested in the hydrogel formulation, but instead in isolation on the HA derivatives. Future work will look at the biocompatibility of cells embedded within the hydrogel matrix and how this effects both biocompatibility and the mechanical strength of the hydrogel. This suggested formulation of a HA-SH: HA-MA blend could be used in many different bioengineering applications due to the ability to tailor the degradation profile. Another limitation of this study was in the confirmation of the presence of the thiolene bond which would be difficult to detect using the methods available. Typically, a thiolene bond would be confirmed by observing the reduction in C═C bonds via methods such as FTIR or NMR, but as this study utilised both methacrylate and thiol, this method would not be sufficient for confirmation. Therefore, assumptions are made based on the physical, chemical and biological characteristics observed through the extensive testing conducted when compared to a control of HA-MA and deionised water, and HA-MA with unmodified HA. Click chemistry by nature occurs reliably where complex systems where characterisation of the resulting bonds would be difficult. Therefore, by implementing controls and comparing the physicochemical and biological responses, it can be shown that the thiol is bonding within the system and the most likely conclusion is via click chemistry formation of thiolene bonds. Depending on the application, whether that is mechanical performance, biocompatibility, or physicochemical properties, the degree of modification and the ratio of thiol to methacrylate can be tuned with relative ease to provide the desired response. Future research will investigate stereolithographic 3D printing of this formulation with an optimal ratio for the control of degradation and cross-linking density and potentially look at hybrid polymer options to increase the mechanical strength of the hydrogel for other applications.

CRediT authorship contribution statement

Ciara Buckley: Synthesis; Methodology; Formal analysis; Investigation; Writing-original draft.

Therese R. Montgomery: Writing-review & editing; Supervision; Conceptualization; Resources.

Tomasz Sank: Investigation; Formal analysis.

Brian Murray: Investigation; Formal analysis.

Cormac Quigley: Investigation; Formal analysis.

Ian Major: Writing-review & editing; Conceptualization; Project administration; Resources; Supervision.

Declaration of competing interest

The authors declare the following financial interests/personal relationships which may be considered as potential competing interests: Ciara Buckley reports financial support was provided by the Irish Research Council.

Data availability

Data will be made available on request.

References

[1] D. Nikitovic, S. Pérez, Preface for the special issue on the exploration of the multifaceted roles of glycosaminoglycans: GAGs, Biomolecules 11 (2021) 1630, https://doi.org/10.3390/biom11111630.
[2] A. Kaul, W.D. Short, S.G. Keswani, X. Wang, Immunologic roles of hyaluronan in dermal wound healing, Biomolecules 11 (2021) 1234, https://doi.org/10.3390/biom11081234.
[3] A. Yasin, Y. Ren, J. Li, Y. Sheng, C. Cao, K. Zhang, Advances in hyaluronic acid for biomedical applications, Front. Bioeng. Biotechnol. 10 (2022), 910290, https://doi.org/10.3389/fbioe.2022.910290.
[4] C. Buckley, E.J. Murphy, T.R. Montgomery, I. Major, Hyaluronic acid: a review of the drug delivery capabilities of this naturally occurring polysaccharide, Polymers 14 (2022) 3442, https://doi.org/10.3390/polym14173442.
[5] R. Ucm, M. Aem, Z. Lhb, V. Kumar, M.J. Taherzadeh, V.K. Garlapati, A.K. Chandel, Comprehensive review on biotechnological production of hyaluronic acid: status, innovation, market and applications, Bioengineered 13 (2022) 9645–9661, https://doi.org/10.1080/21655979.2022.2057760.
[6] C. Winters, F. Zamboni, A. Beaucamp, M. Culebras, M.N. Collins, Synthesis of conductive polymeric nanoparticles with hyaluronic acid based bioactive stabilizers for biomedical applications, Mater. Today Chem. 25 (2022), 100969, https://doi.org/10.1016/j.mtchem.2022.100969.
[7] C. Luo, J. Zhao, M. Tu, R. Zeng, J. Rong, Hyaluronan microgel as a potential carrier for protein sustained delivery by tailoring the crosslink network, Mater. Sci. Eng. C 36 (2014) 301–308, https://doi.org/10.1016/j.msec.2013.12.021.
[8] S.S. Pedrosa, C. Gonçalves, L. David, M. Gama, A novel crosslinked hyaluronic acid nanogel for drug delivery: a novel crosslinked hyaluronic acid …, Macromol. Biosci. 14 (2014) 1556–1568, https://doi.org/10.1002/mabi.201400135.
[9] C. Chircov, A.M. Grumezescu, L.E. Bejenaru, Hyaluronic acid-based scaffolds for tissue engineering, Romanian J. Morphol. Embryol. 59 (2018) 71–76.
[10] A. Fallacara, E. Baldini, S. Manfredini, S. Vertuani, Hyaluronic acid in the third millennium, Polymers 10 (2018) 701, https://doi.org/10.3390/polym10070701.
[11] J. Necas, L. Bartosikova, P. Brauner, J. Kolář, Hyaluronic acid (Hyaluronan): a review, Vet. Med. 53 (2008), https://doi.org/10.17221/1930-VETMED.
[12] P. Wongprasert, C.A. Dreiss, G. Murray, Evaluating hyaluronic acid dermal fillers: a critique of current characterization methods, Dermatol. Ther. 35 (2022), e15453, https://doi.org/10.1111/dth.15453.
[13] P. Snetkov, K. Zakharova, S. Morozkina, R. Olekhnovich, M. Uspenskaya, Hyaluronic acid: the influence of molecular weight on structural, physical, physicochemical, and degradable properties of biopolymer, Polymers (Basel) 12 (2020) E1800, https://doi.org/10.3390/polym12081800.
[14] F. Zamboni, C.K. Wong, M.N. Collins, Hyaluronic acid association with bacterial, fungal and viral infections: can hyaluronic acid be used as an antimicrobial polymer for biomedical and pharmaceutical applications? Bioact. Mater. 19 (2023) 458–473, https://doi.org/10.1016/j.bioactmat.2022.04.023.
[15] C. Ke, L. Sun, D. Qiao, D. Wang, X. Zeng, Antioxidant acitivity of low molecular weight hyaluronic acid, Food Chem. Toxicol. 49 (2011) 2670–2675, https://doi.org/10.1016/j.fct.2011.07.020.
[16] A.R. Shewale, C.L. Barnes, L.A. Fischbach, S.T. Ounpraseuth, J.T. Painter, B. C. Martin, Comparison of low-, moderate-, and high-molecular-weight hyaluronic acid injections in delaying time to knee surgery, J. Arthroplast. 32 (2017) 2952–2957.e21, https://doi.org/10.1016/j.arth.2017.04.041.
[17] C.E. Schanté, G. Zuber, C. Herlin, T.F. Vandamme, Chemical modifications of hyaluronic acid for the synthesis of derivatives for a broad range of biomedical applications, Carbohydr. Polym. 85 (2011) 469–489, https://doi.org/10.1016/j.carbpol.2011.03.019.
[18] G. Huang, J. Chen, Preparation and applications of hyaluronic acid and its derivatives, Int. J. Biol. Macromol. 125 (2019) 478–484, https://doi.org/10.1016/j.ijbiomac.2018.12.074.
[19] F. Zamboni, C. Okoroafor, M.P. Ryan, J.T. Pembroke, M. Strozyk, M. Culebras, M. N. Collins, On the bacteriostatic activity of hyaluronic acid composite films, Carbohydr. Polym. 260 (2021), 117803, https://doi.org/10.1016/j.carbpol.2021.117803.
[20] Z. He, H. Luo, Z. Wang, D. Chen, Q. Feng, X. Cao, Injectable and tissue adhesive EGCG-laden hyaluronic acid hydrogel depot for treating oxidative stress and inflammation, Carbohyd. Polym. 299 (2023), 120180, https://doi.org/10.1016/j.carbpol.2022.120180.
[21] J. Chen, J. Yang, L. Wang, X. Zhang, B.C. Heng, D.-A. Wang, Z. Ge, Modified hyaluronic acid hydrogels with chemical groups that facilitate adhesion to host tissues enhance cartilage regeneration, Bioact. Mater. 6 (6) (2021) 1689–1698, https://doi.org/10.1016/j.bioactmat.2020.11.020.
[22] S. Trombino, C. Servidio, F. Curcio, R. Cassano, Strategies for hyaluronic acid-based hydrogel design in drug delivery, Pharmaceutics 11 (2019) 407, https://doi.org/10.3390/pharmaceutics11080407.
[23] S. Bagheri, Z. Bagher, S. Hassanzadeh, S. Simorgh, S.K. Kamrava, V.T. Nooshabadi, R. Shabani, M. Jalessi, M. Khanmohammadi, Control of cellular adhesiveness in hyaluronic acid-based hydrogel through varying degrees of phenol moiety cross-linking, J. Biomed. Mater. Res. A 109 (5) (2021) 649–658, https://doi.org/10.1002/jbm.a.37049.

[24] G. Abatangelo, V. Vindigni, G. Avruscio, L. Pandis, P. Brun, Hyaluronic acid: redefining its role, Cells 9 (7) (2020) 7, https://doi.org/10.3390/cells9071743.
[25] S. Li, M. Pei, T. Wan, H. Yang, S. Gu, Y. Tao, X. Liu, Y. Zhou, W. Xu, P. Xiao, Self-healing hyaluronic acid hydrogels based on dynamic Schiff base linkages as biomaterials, Carbohydr. Polym. 250 (2020), 116922, https://doi.org/10.1016/j.carbpol.2020.116922.
[26] J.V. Gruber, R. Holtz, J. Riemer, Hyaluronic acid (HA) stimulates the in vitro expression of CD44 proteins but not HAS1 proteins in normal human epidermal keratinocytes (NHEKs) and is HA molecular weight dependent, J. Cosmet. Dermatol. 21 (2022) 1193–1198, https://doi.org/10.1111/jocd.14188.
[27] M.Y. Kwon, C. Wang, J.H. Galarraga, E. Puré, L. Han, J.A. Burdick, Influence of hyaluronic acid modification on CD44 binding towards the design of hydrogel biomaterials, Biomaterials 222 (2019), 119451, https://doi.org/10.1016/j.biomaterials.2019.119451.
[28] Y. Wang, S. Zhang, J. Wang, Photo-crosslinkable hydrogel and its biological applications, Chin. Chem. Lett. 32 (2021) 1603–1614, https://doi.org/10.1016/j.cclet.2020.11.073.
[29] F. Cadamuro, S. Sampaolesi, G. Bertolini, L. Roz, F. Nicotra, L. Russo, Click chemistry protocol for 3D bioprintable elastin−hyaluronic acid hydrogels, ChemNanoMat (2022), e202200508, https://doi.org/10.1002/cnma.202200508 n/a(n/a).
[30] H. Xicoy, B. Wieringa, G.J.M. Martens, The SH-SY5Y cell line in Parkinson's disease research: a systematic review, Mol. Neurodegener. 12 (2017) 10, https://doi.org/10.1186/s13024-017-0149-0.
[31] M. Hai, N. Muja, G.H. DeVries, R.H. Quarles, P.I. Patel, Comparative analysis of Schwann cell lines as model systems for myelin gene transcription studies, J. Neurosci. Res. 69 (4) (2002) 497–508, https://doi.org/10.1002/jnr.10327.
[32] M.-E.F. Hegazy, S. Abdelfatah, A.R. Hamed, T.A. Mohamed, A.A. Elshamy, I. A. Saleh, E.H. Reda, N.S. Abdel-Azim, K.A. Shams, M. Sakr, Y. Sugimoto, P.W. Paré, T. Efferth, Cytotoxicity of 40 egyptian plant extracts targeting mechanisms of drug-resistant cancer cells, Phytomedicine 59 (2019), 152771, https://doi.org/10.1016/j.phymed.2018.11.031.
[33] N.J. Leigh, P.L. Tran, R.J. O'Connor, M.L. Goniewicz, Cytotoxic effects of heated tobacco products (HTP) on human bronchial epithelial cells, Tob. Control. 27 (Suppl 1) (2018) s26–s29, https://doi.org/10.1136/tobaccocontrol-2018-054317.
[34] X. Qie, W. Chen, M. Zeng, Z. Wang, J. Chen, H.D. Goff, Z. He, Interaction between β-lactoglobulin and chlorogenic acid and its effect on antioxidant activity and thermal stability, Food Hydrocoll. 121 (2021), 107059, https://doi.org/10.1016/j.foodhyd.2021.107059.
[35] I. Rahman, A. Kode, S.K. Biswas, Assay for quantitative determination of glutathione and glutathione disulfide levels using enzymatic recycling method, Nat. Protoc. 1 (6) (2006) 3159–3165, https://doi.org/10.1038/nprot.2006.378.
[36] M.H.M. Oudshoorn, R. Rissmann, J.A. Bouwstra, W.E. Hennink, Synthesis of methacrylated hyaluronic acid with tailored degree of substitution, Polymer 48 (7) (2007) 1915–1920, https://doi.org/10.1016/j.polymer.2007.01.068.
[37] Y. Ni, Z. Tang, W. Cao, H. Lin, Y. Fan, L. Guo, X. Zhang, Tough and elastic hydrogel of hyaluronic acid and chondroitin sulfate as potential cell scaffold materials, Int. J. Biol. Macromol. 74 (2015) 367–375, https://doi.org/10.1016/j.ijbiomac.2014.10.058.
[38] E. Shirzaei Sani, R. Portillo-Lara, A. Spencer, W. Yu, B.M. Geilich, I. Noshadi, T. J. Webster, N. Annabi, Engineering adhesive and antimicrobial hyaluronic acid/elastin-like polypeptide hybrid hydrogels for tissue engineering applications, ACS Biomater. Sci. Eng. 4 (7) (2018) 2528–2540, https://doi.org/10.1021/acsbiomaterials.8b00408.
[39] J. Li, Y. Xu, Y. Wang, Y. Hsu, P. Wang, J. Li, The role of hyaluronidase for the skin necrosis caused by hyaluronic acid injection-induced embolism: a rabbit auricular model study, Aesthet. Plast. Surg. 43 (5) (2019) 1362–1370, https://doi.org/10.1007/s00266-019-01398-2.
[40] X. Jin, S. Asghar, M. Zhang, Z. Chen, L. Huang, Q. Ping, Y. Xiao, N-acetylcysteine modified hyaluronic acid-paclitaxel conjugate for efficient oral chemotherapy through mucosal bioadhesion ability, Colloids Surf B Biointerfaces 172 (2018) 655–664, https://doi.org/10.1016/j.colsurfb.2018.09.025.
[41] R.W. Eyler, E.D. Klug, Floyd Diephuis, Determination of degree of substitution of sodium carboxymethylcellulose, Anal. Chem. 19 (1) (1947) 24–27, https://doi.org/10.1021/ac60001a007.
[42] A. Mehring, N. Erdmann, J. Walther, J. Stiefelmaier, D. Strieth, R. Ulber, A simple and low-cost resazurin assay for vitality assessment across species, J. Biotechnol. 333 (2021) 63–66, https://doi.org/10.1016/j.jbiotec.2021.04.010.
[43] R. Chelliah, D.-H. Oh, Screening for anticancer activity: neutral red uptake assay, in: D. Dharumadurai (Ed.), Methods in Actinobacteriology, Springer, US, 2022, pp. 431–433, https://doi.org/10.1007/978-1-0716-1728-1_56.
[44] K. Präbst, H. Engelhardt, S. Ringgeler, H. Hübner, Basic colorimetric proliferation assays: MTT, WST, and resazurin, in: D.F. Gilbert, O. Friedrich (Eds.), Cell Viability Assays: Methods and Protocols, Methods in Molecular Biology, Springer, New York, NY, 2017, pp. 1–17, https://doi.org/10.1007/978-1-4939-6960-9_1.
[45] G. Repetto, A. del Peso, J.L. Zurita, Neutral red uptake assay for the estimation of cell viability/cytotoxicity, Nat. Protoc. 3 (2008) 1125–1131, https://doi.org/10.1038/nprot.2008.75.
[46] Sara Howe, Sheldon M. Newman, Jeffrey W. Stansbury, Bond Strength of Thiol-ene/Methacrylate Composite Restorative Materials IADR Abstract Archives, Retrieved February 8, 2023, from, https://iadr.abstractarchives.com/abstract/2008Dallas-101057/bond-strength-of-thiol-enemethacrylate-composite-restorative-materials, 2018.
[47] S. Singh, A.K. Rai, R. Prakash Tewari, Recent advancement in hyaluronic acid-based hydrogel for biomedical engineering application: A mini-review, Materials Today: Proceedings. (2023), https://doi.org/10.1016/j.matpr.2022.12.208.
[48] P.N. Dave, A. Gor, Chapter 3 - natural polysaccharide-based hydrogels and nanomaterials: recent trends and their applications, in: C. Mustansar Hussain (Ed.), Handbook of Nanomaterials for Industrial Applications, Micro and Nano Technologies, Elsevier, 2018, pp. 36–66, https://doi.org/10.1016/B978-0-12-813351-4.00003-1.
[50] E. Daminato, G. Bianchini, V. Causin, New directions in aesthetic medicine: a novel and hybrid filler based on hyaluronic acid and lactose modified chitosan, Gels 8 (5) (2022) 326, https://doi.org/10.3390/gels8050326.